Improved Stability of Running over Unknown Rough Terrain via Prescribed Energy Removal

Bruce Miller, Ben Andrews, and Jonathan E. Clark

Abstract. The speed and maneuverability at which legged animals can travel through rough and cluttered landscapes has provided inspiration for the pursuit of legged robots with similar capabilities. Researchers have developed reduced-order models of legged locomotion and have begun investigating complementary control strategies based on observed biological control schemes. This study examines a novel control law which prescribes a feed-forward actuation scheme in which energy is actively removed during a portion of each stride to maximize stability. The behavior of this approach is demonstrated on a dynamic running platform while traversing a track with unexpected alterations in terrain height. Results indicate that this novel control approach provides greater stability for a single-legged hopping robot than more traditional control methods.

1 Introduction

The ability of legged animals to adapt effortlessly to variations in terrain has inspired scientists and roboticists to study and build legged locomoters. Running models such as the Spring Loaded Inverted Pendulum (SLIP) model have been utilized to help researchers understand the fundamentals of biological legged locomotion [Alexander and Vernon(1975)]. While the equations of motion governing this model are simple, they are capable of reproducing the center of mass trajectory and ground reaction force profiles observed in a wide variety of running animals [Blickhan and Full(1993)]. With the insights gained from studying 'templates' [Full and Koditschek(1999)], such as the SLIP model, researchers have begun to

Bruce Miller · Ben Andrews · Jonathan Clark
FAMU & FSU College of Engineering, Tallahassee, FL, USA
e-mail: jeclark@fsu.edu

O. Khatib, V. Kumar, and G. Sukhatme (eds.), *Experimental Robotics*,
Springer Tracts in Advanced Robotics 79,
DOI: 10.1007/978-3-642-28572-1_26,

create legged robotic platforms capable of fast, stable locomotion [Raibert(1986), Altendorfer et al(2001), Cham et al(2002)].

Recent studies have investigated how SLIP-like dynamics are maintained in non-energetically conservative systems. Investigations such as the drop-step perturbation studies performed on guinea fowl have demonstrated that stable locomotion can be maintained in animals when an unknown obstacle is encountered with minimal neural feedback [Daley and Biewener(2006)]. These studies suggest that the intrinsic properties of the leg and the use of muscles to actively remove and add energy, rather than only add energy to compensate for system losses, facilitated the recovery to a stable gait.

Previous research on hopping robots has focused mainly on flat terrain, terrain with known obstacles, and/or robots with numerous complex sensors and computationally intensive control algorithms. However, in order to further exploit the advantages of legged locomotion, it is necessary to be able to negotiate unknown, rough terrain. Furthermore, if autonomy is desired, minimal sensing and computation become attractive traits as they minimize the space and computing power required to maintain stable locomotion, which can instead be utilized towards other tasks.

Simple, clock-driven controllers have accomplished this by means of passive stabilization, relying on the interplay of feed-forward actuation, leg impedance, and ground contact to recover from perturbations. By adding a minimal amount of sensing (timing of ground contact), Schmitt and Clark have shown that a guinea fowl-inspired prescribed energy removal scheme can improve the system's stability–at least in simulation [Schmitt and Clark(2009)].

In this work, we test the efficacy of the feed-forward active energy removal control strategy on a minimal-sensing, single-legged hopping robot. To provide context, these results are compared to a traditional controller which only adds energy during stance [Raibert(1986)]. These experiments show that the active removal of energy can result in a greater ability to traverse unknown, rough terrain with minimal sensing of the robot's state and surrounding environment.

2 Modeling and Control

2.1 Biological Inspiration

Legged locomotion over rough terrain has traditionally been considered a computationally intensive task, requiring complex leg coordination schemes and sensory modes [Hodgins and Raibert(1991), Nelson and Quinn(1999)]. However, recent animal locomotion studies with cockroaches and guinea fowl have provided insight into computationally and sensorially inexpensive mechanisms to respond to terrain variation [Sponberg and Full(2008), Daley and Biewener(2006)]. The results from these studies suggest that feed-forward leg actuation schemes can be utilized to reject small perturbations so that high-level reflexes are only necessary to overcome

large or persistent disturbances. The following subsections briefly describe the reduced order system model and the controller which has been developed to function in a similar fashion to the feed-forward behavior described above. A more conventional controller, first used by Raibert, is also presented as it was implemented on the physical system as a comparison point.

2.2 Reduced Order Modeling of Legged Locomotion

The Spring Loaded Inverted Pendulum (SLIP) model is commonly used as a template for legged locomotion. In the conservative SLIP template, the body is modeled as a point mass m mounted on a massless leg of variable length ζ with an axially elastic, laterally rigid linear spring that has a spring constant k and a force-free length of l_o. The angle of the leg θ is defined from the vertical axis measured positive in a clock-wise fashion. For the nonconservative model, linear and rotational damping, b_L and b_R, respectively, are also added to the model, as shown in Fig. 1a. Locomotion is constrained to occur within the sagittal plane, and each stride is comprised of a stance and flight phase, as depicted in Fig. 1b.

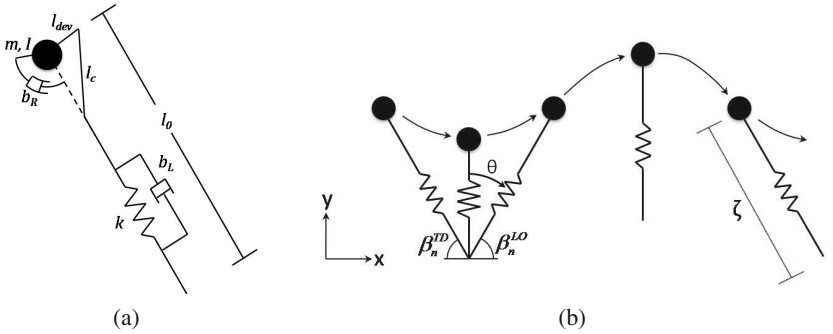

Fig. 1 The SLIP Model. (a) Schematic of the leg and body and (b) the trajectory of the model over the course of one stride.

The stance phase begins when the leg, extended to its force-free length l_o, touches the ground at an angle β_n^{TD}, measured positive in a clockwise fashion from the foot pivot point. For the purposes of this discussion, subscripts denote the stride number, while superscripts identify variables at leg touch-down (TD) and lift-off (LO) events. The foot pivot point is modeled as a moment-free pin joint and remains fixed for the duration of the stance phase. The body begins the stance phase with horizontal and vertical velocities, $\dot{x}$ and $\dot{y}$, respectively. The horizontal and vertical velocities can be mapped to the variable leg length and leg angle as shown in (1) and (2).

$$\zeta = \sqrt{x^2 + y^2}, \quad \dot{\zeta} = \frac{x\dot{x} + y\dot{y}}{\sqrt{x^2 + y^2}} \tag{1}$$

$$\theta = \arctan\left(\frac{x}{y}\right), \quad \dot{\theta} = \frac{x\dot{y} - x\dot{y}}{x^2 + y^2} \tag{2}$$

The body moves forward under the influence of gravity and its own momentum, compressing and expanding the elastic spring, as governed by (3) and (4), until the ground reaction force returns to zero. At this instant, the leg becomes airborne at an angle β_n^{LO}, measured positive in a counter-clockwise fashion from the foot pivot, and the body undergoes a flight phase governed by simple ballistic dynamics. The flight phase ends when the leg next touches down, with the leg extended to the force-free length l_o and an at angle β_{n+1}^{TD}.

$$\ddot{x} = \frac{k}{m}(l_0 - \zeta)\sin\theta - \frac{b_L}{m}\dot{\zeta}\sin\theta - \frac{b_R}{m\zeta}\dot{\theta}\cos\theta \tag{3}$$

$$\ddot{y} = \frac{k}{m}(l_0 - \zeta)\cos\theta - \frac{b_L}{m}\dot{\zeta}\cos\theta + \frac{b_R}{m\zeta}\dot{\theta}\sin\theta - g \tag{4}$$

2.3 Control Approaches

While many control approaches have been developed for implementation on SLIP-like running robots, two are considered in the context of this study. The first controller, 'Active Energy Removal' (AER), was initially proposed by Schmitt [Schmitt(2007)] and is being implemented for the first time on a physical system. The second controller, 'Fixed Thrust' (FT), is based on a common control strategy in which energy is added after maximum compression to counteract system losses and is used to evaluate the effectiveness of the AER controller.

2.3.1 Active Energy Removal

The 'Active Energy Removal' controller was developed as a result of studies on guinea fowl in which it was shown that when encountering an unexpected drop, the animal would utilize posture-dependent leg actuation to actively brake itself during the next stride [Daley and Biewener(2006)]. Another study with cockroaches showed that when placed in an environment with obstacles distributed in a random array and up to three times the hip height, the insect could still move at 80% of its unobstructed speed [Sponberg and Full(2008)]. Furthermore, it was observed that even for steps in which the leg does not contact the ground (i.e. due to a significant drop), leg progression was not stopped to search for a foothold, but rather continued along a similar trajectory as if it had encountered the ground, indicating that a feed-forward trajectory was likely prescribed for the leg.

Schmitt [Schmitt(2007)] hypothesized a controller based on these results and examined it when used in conjunction with a conservative SLIP model. For the controller, leg angle changes at touch-down were determined via feedback while the leg length actuation was specified in a feed-forward manner. Simulations demonstrated that this control strategy would allow for the recovery from terrain drops of up to 40% of the hip height, similar to the performance seen in guinea fowl [Daley and Biewener(2006)]. The robust locomotion performance evidenced by use of these simple control strategies, both in animals and reduced order model simulations, motivates the current investigation into their performance in a robotic instantiation.

As mentioned previously, Schmitt introduced a scheme to modulate the system energy during stance by varying the force free leg length, l_0, as:

$$l_0 = l_{nom} - l_{dev} \sin\left(\frac{\pi t}{t_{des}}\right), \tag{5}$$

where l_{nom} represents the nominal leg length, l_{dev} is maximum deviation from the nominal leg length, and t_{des} is a timing based mechanism for leg actuation. In this formulation, t denotes the time elapsed from the beginning of the current stance phase, such that $t = 0$ at the beginning of each stance (i.e. when touch-down occurs).

In this actuated formulation, energy is removed from the system by rotating the crank to shorten the force-free leg length during leg compression. It is then returned to the system during leg extension by continuing to rotate the crank to lengthen the force-free leg length. For a periodic gait, gait symmetry in ζ and $\dot{\zeta}$ about mid-stance ensures that the energy absorbed during the first half of the stance phase equals that added during the latter half, such that the energy at lift-off equals that at touchdown. However, such gait symmetry is destroyed in the presence of external perturbations, such as those that would naturally occur when running over rough terrain. In these instances, the leg lift-off event can occur earlier or later than that of the periodic gait, thereby directly affecting the amount of energy added back into the system during the extension phase. The novelty of this strategy for controlling the system energy is that the leg actuation is prescribed in a feed-forward fashion and does not change in response to transient variations in the environment. By using an actuation strategy which actively removes energy at the beginning of stance, stability and robustness can be improved with minimal computational power, though at the cost of a decreased energy efficiency.

In addition to the leg actuation protocol in 5, an adaptive leg touch-down angle control law was implemented and is defined as:

$$\beta_{n+1}^{TD} = \beta_n^{LO} + c\left(\beta_n^{TD} - \beta_{des}^{TD}\right), \tag{6}$$

where c is a dimensionless control parameter. This control law was developed to improve the stability of the heading angle at touch-down and it has been shown that with an appropriate choice for c, most gaits can be stabilized [Schmitt(2006)].

2.3.2 Fixed Thrust

Raibert and his colleagues at CMU and at the MIT Leg Lab pioneered the idea of decoupled control laws in running robots. To achieve stable locomotion, control laws were developed that separately stabilized each of the following states: apex height, forward velocity, and body attitude. Even though motions in the physical system were dynamically coupled, Raibert assumed that the control laws could be designed and governed independently [Raibert(1986)].

The apex height control law, comparable to the energy incorporation control law for AER, added energy to the system by providing an impulse of a fixed amount of energy into the system each stride at the point of maximum leg compression via a pneumatic piston. This fixed energy addition counteracted frictional losses in the system and resulted in a steady state hop height proportional to the amount of energy added.

Forward velocity was controlled by utilizing a feedback control law to calculate the upcoming touch-down angle of the leg. Raibert designed this leg angle control algorithm to place the foot pivot at the predicted midpoint of the upcoming stance, as defined by:

$$\beta_{n+1}^{TD} = \arccos\left(\left(\frac{\dot{x}T_s}{2l_0}\right) + K_{\dot{x}}\left(\frac{\dot{x} - V_{des}}{l_0}\right)\right), \tag{7}$$

where $\dot{x}$ is the forward velocity from the previous stance, T_s is the previous stance time, V_{des} is a parameter that influences forward velocity, $K_{\dot{x}}$ is a controller gain selected to maximize stability, and l_0 is the nominal leg length [Raibert(1986)]. The body attitude control law utilized a gyroscope and hip torques to maintain the body in an upright position; however, this control law is neglected in the current study, because the body attitude of the physical robot is held constant by a boom.

While this instantiation of the Fixed Thrust controller was one of Raibert's early formulations, it is one that can be adapted to the actuation and sensing capabilities of our hopping robot. For the apex height control, a crank-coupler mechanism was substituted for pneumatic actuation and energy input was controlled by rotating the crank to a desired angle C_{des} as quickly as possible. Also, instead of actuating at maximum compression, actuation was initiated when the hip angle became zero (i.e. the leg was vertical) since a leg length sensor was not used on the robot. The forward velocity control law was modified so only the touch-down and lift-off angles and stance time would be needed. The forward velocity $\dot{x}$ was approximated as:

$$\dot{x} = \frac{l_0\left(\cos\beta_n^{TD} + \cos\beta_n^{LO}\right)}{T_s} \tag{8}$$

under the assumption that the leg length was approximately equal to the rest leg length at touch-down and lift-off and that the average forward velocity during stance

was the same as the average forward velocity during flight. Using this definition for $\dot{x}$, the forward velocity control law can be rewritten as:

$$\beta_{n+1}^{TD} = \arccos\left(\left(\frac{\cos\beta_n^{TD} + \cos\beta_n^{LO}}{2}\right) + K_{\dot{x}}\left(\frac{\cos\beta_n^{TD} + \cos\beta_n^{LO}}{T_s} - \frac{V_{des}}{l_0}\right)\right). \quad (9)$$

3 Simulation

To model the physical robot, a dynamic simulation was implemented in MATLAB using the Runge-Kutta integrator *ode*45 in which the robot was modeled as a SLIP-like runner using the formulation described in Sec. 2.2. This simulation was used to search for desirable gait parameters to be used on the physical system which provided the quickest recovery from step perturbations. To determine the recovery rate, fixed points were first found using a Newton-Raphson search. Raised and lowered step disturbances of $2cm$ to $10cm$ were then applied to the simulation and the number of hops required for the system to settle was determined for each parameter set. The number of hops to settling was computed as the average number of hops before both apex height and forward velocity returned to within 10% of their steady steady value for all step heights. Using this metric as the objective function, desired gait parameters were determined using a brute force search over the parameter range. For the AER controller, the free parameters were t_{des}, β_{des}^{TD}, and c. For the FT controller, the free parameters were C_{des}, V_{des}, and $K_{\dot{x}}$.

Once the number of hops to settling had been found for the parameter sets, constraints were established to limit the selection of gaits to a desired range. In this investigation, the clearance percentage $\%_{clear}$ was used to constrain gaits, which is defined as the fraction of steps of a given height the robot would clear if placed randomly within one stride length, as shown below:

$$\%_{clear} = \sqrt{\frac{y_{apex} - y_{step}}{y_{apex}}}, \quad (10)$$

where y_{apex} is the steady-state apex height and y_{step} is the height of the step. The minimum bound for clearance percentage was chosen to be 65% to select for gaits that would typically clear the step. The maximum bound was chosen to be 75% to constrain apex heights to a similar range such that gaits would not be chosen to which the step was only a small perturbation. The step height was chosen as $8cm$, and by using (10), the range for apex height can be found as $13.8 - 18.3cm$, which corresponds to the step being $44\% - 58\%$ of the apex height. The gaits and corresponding settling periods were then compiled and analyzed, as discussed in Sec. 5.2.

4 Physical Platform

In order to evaluate the effectiveness of the proposed leg control approaches, a single-legged hopping robot capable of sagittal plane locomotion was required. The platform needed to be able to extend and contract the leg length in a sinusoidal

fashion and to actuate the leg to a specified angle with respect to the ground. The body was designed such that the center of mass coincided with the hip joint and the moment of inertia was minimal to preserve the approximation of the body as a point mass. Additionally, sensors were added to allow the robot to sense touch-down and lift-of events. The physical design was chosen to match the SLIP model, presented in Sec. 2.2, as closely as possible. Finally, the leg was scaled to 30% of the length of a human leg, such that the dynamic characteristics would be maintained [Clark et al(2006)] while making the size more manageable, as shown in Table 1.

Table 1 Dynamically scaled parameters for the robot

Property	Human Scale	Scaling Factor	30% Scale	Robot Values
Mass	$80kg$	α_L^3	$2.16kg$	$2.11kg$
Leg Stiffness	$20000\frac{N}{m}$	α_L^2	$1800\frac{N}{m}$	$1919\frac{N}{m}$
Leg Length	$1m$	α_L	$0.3m$	$0.298m$

The robot was designed to run around a circular track attached to a boom which rotates around a center pivot. This setup restricts the robot to a spherical workspace around the center pivot. An aluminum tube with an outer diameter of $5.7cm$, walls $1mm$ thick, and $1.19m$ in length was chosen as the boom. This size was selected to minimize flexing of the boom and to allow the hip motor to be mounted within the boom. A tiled floor with a hard carpet surface for traction was used for the ground level track. Steps were made out of wood using the same carpet as a surface for the raised steps.

To actuate the hip, a DC brushed motor (Faulhaber 3257-024CR) was mounted in the boom and attached to the leg housing. To allow the variation of the force-free leg length, a crank slider mechanism was utilized. A second DC brushed motor (same as the hip) was set at the top of the leg housing to turn a crank l_{dev}, which is coupled to a linkage arm l_{cup}, as shown in Fig. 2a. The leg length l_{nom} was defined as the leg length when the slider, and consequently the force-free leg length, was halfway between its shortest and longest positions. A fixed linear bearing was set at the bottom of the slider with a movable $1/4''$ rod passing through it. The rod passed through the center of the leg spring and attached to the foot, resulting in a 'coilover' spring configuration. The 'toe' was designed as an aluminum hemisphere with a linear slide that attached to the bottom of the foot. The toe served as the point of contact with the ground during locomotion. The sensors used for control include an embedded encoder in each of the motors as well as a simple plunger type switch, housed in the foot, to act as a ground contact sensor. Additionally, an encoder was placed on the boom to record its angle from the horizontal and on the center pivot to record the angular travel along the track, though the data from these encoders was used solely for analytical purposes.

An electronics system was developed for onboard control of the robot. A Gumstix Basix board running a Linux operating system was used as the mainboard, with

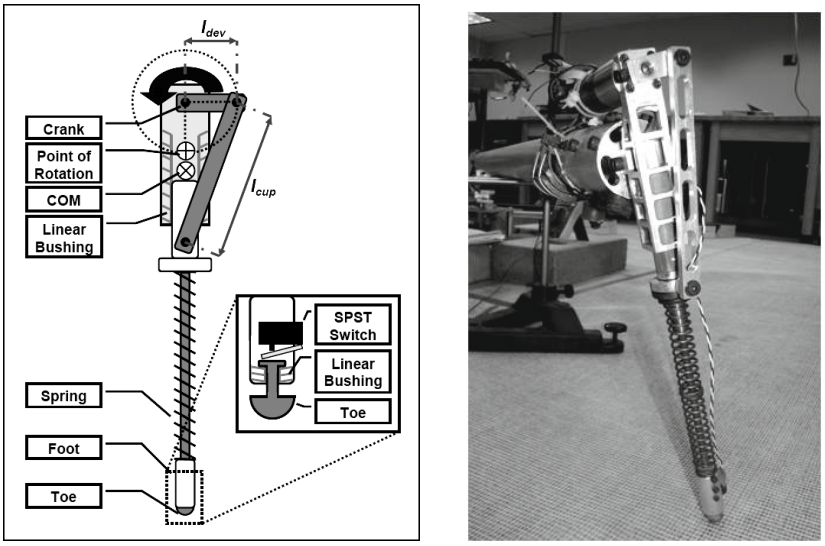

(a) (b)

Fig. 2 (a) A diagram of the robot leg and (b) a photograph of the single-legged hopping robot

a 400*Mhz* Intel PXA255 processor, 64*MB* of RAM, and Bluetooth wireless connectivity. Two dual quadrature decoder chips (Avago HCTL-2032) were used to collect encoder data from four encoders (one for the hip motor, one for the crank motor, one for the boom angle from the horizontal, and one for the boom angle along the track). Two high power motor drivers (Pololu 36v9) were used to drive the two motors, each capable of outputting 50*V* at up to 9*A* continuously.

5 Experimental Results

5.1 Model-Robot Comparison

Three sets of gait parameters were selected using the controller parameter selection process (Sec. 3) to be implemented on the robot. Each gait was run on both the carpeted ground and on a track made of the steps to be used as perturbations to determine the steady-state behavior. Both surfaces were characterized to account for differences in surface stiffness and damping between the two levels. The gaits were then compared to simulation results to determine the accuracy of the simulation using two metrics. The first metric compared the steady-state behavior of the robot to the simulation. For this comparison, the apex height, forward velocity, and touch-down and lift-off angles were considered. The correlation of the simulation to experimental data was determined by the percent differences and the number of standard deviations of the experimental data separating the results. The second metric examined the difference in apex height and forward velocity of the robot and

Table 2 Comparison of simulated and experimental results for an AER controller at steady-state.

Property	Simulation	Robot AVG	Robot STD	% Difference
Touch-Down Angle	8.11°	7.80°	0.893°	3.9%
Lift-Off Angle	13.39°	13.20°	1.12°	1.4%
Apex Height	15.4cm	16.9cm	0.85cm	9.9%
Forward Velocity	0.858$\frac{m}{s}$	0.856$\frac{m}{s}$	0.031$\frac{m}{s}$	0.3%

Table 3 Comparison of simulated and experimental results for a FT controller at steady-state.

Property	Simulation	Robot AVG	Robot STD	% Difference
Touch-Down Angle	9.08°	8.75°	0.685°	3.6%
Lift-Off Angle	16.38°	15.56°	0.897°	5.0%
Apex Height	13.7cm	14.6cm	0.57cm	6.5%
Forward Velocity	1.081$\frac{m}{s}$	1.098$\frac{m}{s}$	0.062$\frac{m}{s}$	1.6%

simulation in the individual strides following a step perturbation. The root centered mean squared error (RCMSE) [Petzoldt et al(2007)] between the simulation and experiment was calculated and compared to the standard deviation of the robot data during the steps following a perturbation.

According to both metrics, the simulation showed a relatively strong correlation to the robot data. A comparison of the first method for two of the gaits, one using each controller, is shown in Tables 2 and 3. For both of these gaits, no difference greater than two standard deviations or 10% of the data was seen. Other gaits showed similar results, with the simulation always matching within four standard deviations and 20% of the robot data. A comparison for the second method is shown in Figs. 3 and 4. Steps both up and down were examined and the RCMSE was found to be less than two standard deviations for all of the gaits. While these results show that some discrepancies exist between the simulation and physical robot, it also demonstrates evidence that the simulation can provide a preliminary estimate of the robot behavior.

5.2 Controller Comparison

Once the simulation results had been verified, data from the perturbation trials was used to calculate the number of steps to settling. For the purpose of this study, the gait was considered to have settled when it returned within 10% of its steady-state value for both apex height and forward velocity. The settling bounds were chosen to be slightly larger than twice the steady-state standard deviation for both apex height and forward velocity. This minimized the chance that a gait would not converge due to noise but is still sufficiently smaller than the step height to ensure that a significant recovery was made before considering the gait to have settled. Figure 5

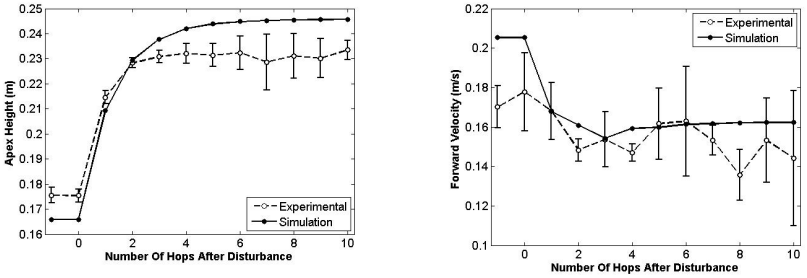

(a) Apex Height Response (b) Forward Velocity Response

Fig. 3 Response of the robot to a raised step perturbation in simulation and experimentally using an AER controller.

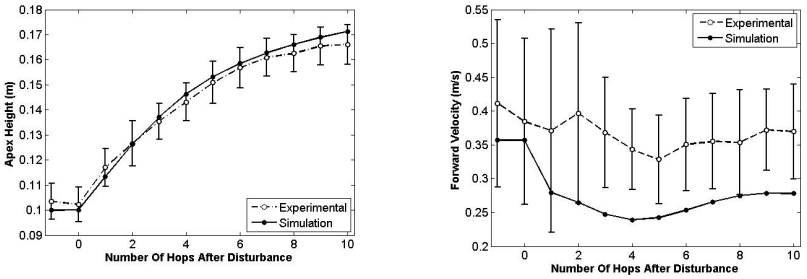

(a) Apex Height Response (b) Forward Velocity Response

Fig. 4 Response of the robot to a raised step perturbation in simulation and experimentally using a FT controller.

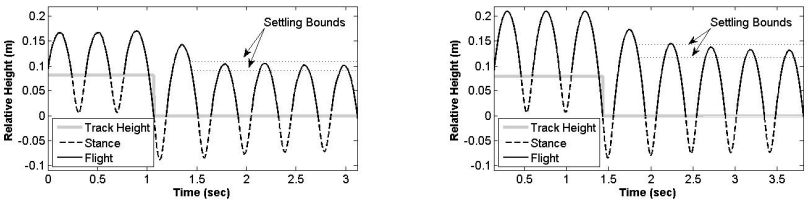

(a) Experimental Results (b) Simulation Results

Fig. 5 Apex height data for the robot encountering a drop-step perturbation.

shows both experimental (Fig. 5a) and simulation (Fig. 5b) apex height data of the robot reaching the drop step perturbation and stabilizing to its steady-state value.

The results calculated for the settling time both experimentally and for optimal gaits in simulation are shown in Fig. 6. The simulated results were obtained by forward simulation over raised and lowered steps of $2cm$ to $10cm$ and averaging the number of hops required to settle, as described above, while the robot data was

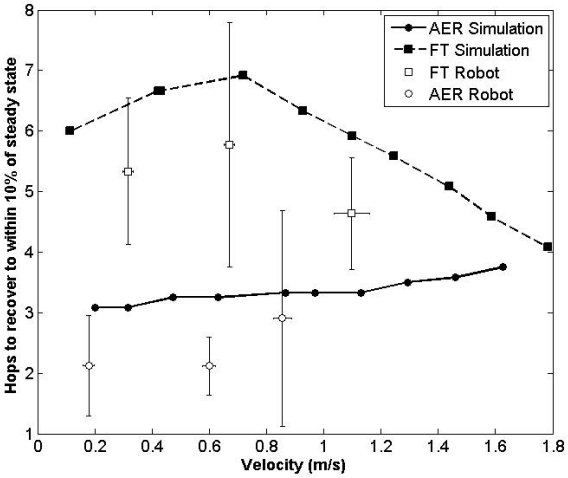

Fig. 6 Number of hops to settling as a function of forward velocity. Experimental and simulation results are shown for both AER and FT controllers.

obtained by running multiple trials over steps up and down of $8cm$ and averaging the results. From the simulation data, two trends appear evident. First, the average number of hops to settling of the AER controller stays relatively unchanged across the sampled velocity range, rising only slightly from 3.083 hops to 3.75 hops. Second, the number of hops to settling for the FT controller increases as the velocity rises from $0.1\frac{m}{s}$ to $0.75\frac{m}{s}$ and then decreases as the velocity continues to increase until it reaches about the same level as the AER controller. The robot data follows a roughly similar trend, with the AER controlled gaits all maintaining mean settling times between two and three steps while the FT controlled gaits were always slower to recover and took longer to stabilize at slow speeds than at the high speed gait.

6 Conclusion

The results shown above establish the effectiveness of a feed-forward active energy removal scheme for the use on a single-legged hopping robot. For the velocity range examined, the AER controller showed consistent, rapid recovery from step perturbations. The comparison with a fixed thrust controller demonstrates the decrease in recovery time achieved through the use of this controller, especially when running at low speeds. These results suggest that when stability is a critical requirement, such as when traversing unknown, irregular terrain, the use of an active energy removal control scheme will yield superior performance and should be preferred to an otherwise similar controller which only adds energy. Further testing will investigate running using prescribed active energy removal over natural terrains (i.e. grass, sand, dirt, etc.) as well as implementing the control strategy on a multi-legged system.

Additionally, the efficacy of the AER controller should be examined as the system and surface damping is varied to determine when this controller is most beneficial.

While the metric used to determine stability in this study, the number of steps to recovery, confirms the efficacy of the AER controller, as the sole indicator of stability, its insightfulness is limited. This is primarily because it gives no indication of how perturbations of different sizes will affect the stability and it requires that the robot have sufficient time after a perturbation to return to steady state without encountering another obstacle. Further studies need to be conducted to determine a metric which can be easily implemented on a physical system, provides insight into both the rate of recovery and the range of recovery, and can be calculated from only a few steps following a disturbance.

Acknowledgments. The authors would like to thank John Schmitt for his assistance. This work was supported in part by NSF CMMI-0826137.

References

[Alexander and Vernon(1975)] Alexander, R.M., Vernon, A.: Mechanics of hopping by kangaroos (macropodidae). Journal of Zoology 177, 265–303 (1975)

[Altendorfer et al(2001)] Altendorfer, R., Moore, N., Komsuoglu, H., Buehler, M., Brown, H.B.J., Mc- Mordie, D., Saranli, U., Full, R., Koditschek, D.E.: Rhex: A biologically inspired hexapod runner. Autonomous Robots 11(3), 207–213 (2001)

[Blickhan and Full(1993)] Blickhan, R., Full, R.: Similarity in multilegged locomotion - bouncing like a monopode. Journal of Comparative Physiology A-Sensory Neural and Behavioral Physiology 173(5), 509–517 (1993)

[Cham et al(2002)] Cham, J.G., Bailey, S.A., Clark, J.E., Full, R.J., Cutkosky, M.R.: Fast and robust: Hexapedal robots via shape deposition manufacturing. International Journal of Robotics Research 21(10) (2002)

[Clark et al(2006)] Clark, J., Goldman, D., Chen, T., Full, R., Koditschek, D.: Towards vertical dynamic climbing. In: Proceedings of the 9th International Conference on Climbing and Walking Robots, Brussels, Belgium (2006)

[Daley and Biewener(2006)] Daley, M.A., Biewener, A.A.: Running over rough terrain reveals limb control for intrinsic stability. Proceedings of the National Academy of Sciences of the United States of America 103(42), 15,681–15,686 (2006)

[Full and Koditschek(1999)] Full, R., Koditschek, D.: Templates and anchors: Neuromechanical hypotheses of legged locomotion on land. Journal of Experimental Biology 202(23), 3325–3332 (1999)

[Hodgins and Raibert(1991)] Hodgins, J., Raibert, M.: Adjusting step length for rough terrain locomotion. IEEE Transactions on Robotics and Automation 7(3), 289–298 (1991)

[Nelson and Quinn(1999)] Nelson, G., Quinn, R.: Posture control of a cockroach-like robot. IEEE Control Systems Magazine 19(2), 9–14 (1999)

[Petzoldt et al(2007)] Petzoldt, T., van den Boogaart, K.G., Jachner, S.: Statistical methods for the qualitative assessment of dynamic models with time delay (r package qualv). Journal of Statistical Software 22(8) (2007)

[Raibert(1986)] Raibert, M.H.: Legged robots that balance. Massachusetts Institute of Technology, Cambridge (1986)

[Schmitt(2006)] Schmitt, J.: A simple stabilizing control for sagittal plane locomotion. Journal of Computational and Nonlinear Dynamics 1(4), 348–357 (2006)

[Schmitt(2007)] Schmitt, J.: Incorporating energy variations into controlled sagittal plane locomotion dynamics. In: Proceedings of the ASME International Design, Engineering and Technical Conference (2007)

[Schmitt and Clark(2009)] Schmitt, J., Clark, J.: Modeling posture-dependent leg actuation in sagittal plane locomotion. Bioinspiration & Biomimetics 4(4) (2009)

[Sponberg and Full(2008)] Sponberg, S., Full, R.J.: Neuromechanical response of musculoskeletal structures in cockroaches during rapid running on rough terrain. Journal of Experimental Biology 211(3), 433–446 (2008)